Electronic Supplementary Material (ESI) for RSC Advances.

Nanostructured carbon-metal hybrid aerogels from bacterial cellulose

Bernd Wicklein[a,*], Judith Arranz[a], Alvaro Mayoral[b], Pilar Aranda[a], Yves Huttel[a], Eduardo Ruiz-Hitzky[a]

[a]Instituto de Ciencia de Materiales de Madrid, CSIC, c/ Sor Juana Inés de la Cruz 3, 28049 Madrid, Spain
[b] Laboratorio de Microscopías Avanzadas, Instituto de Nanociencia de Aragón, Universidad de Zaragoza, c/ Mariano Esquillor, Edificio I+D, 50018, Zaragoza, Spain

*Author for correspondence. E-mail: bernd@icmm.csic.es

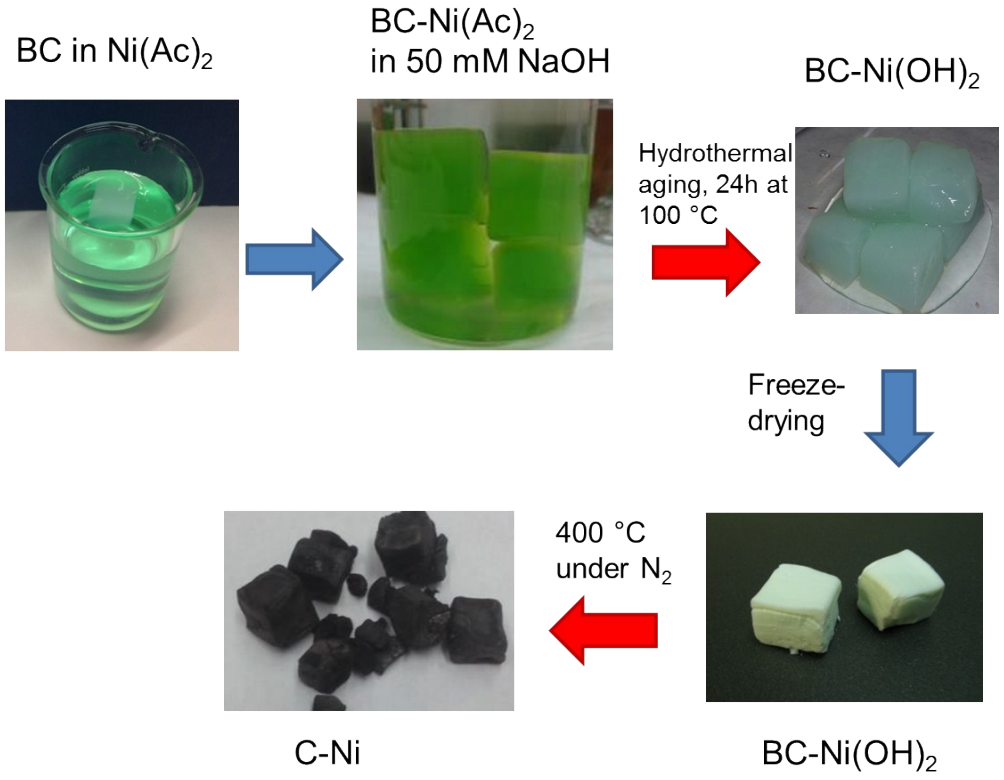

Figure S1: Experimental procedure for the synthesis of carbon-nickel (C-Ni) from pyrolysis of BC-Ni(OH)$_2$.

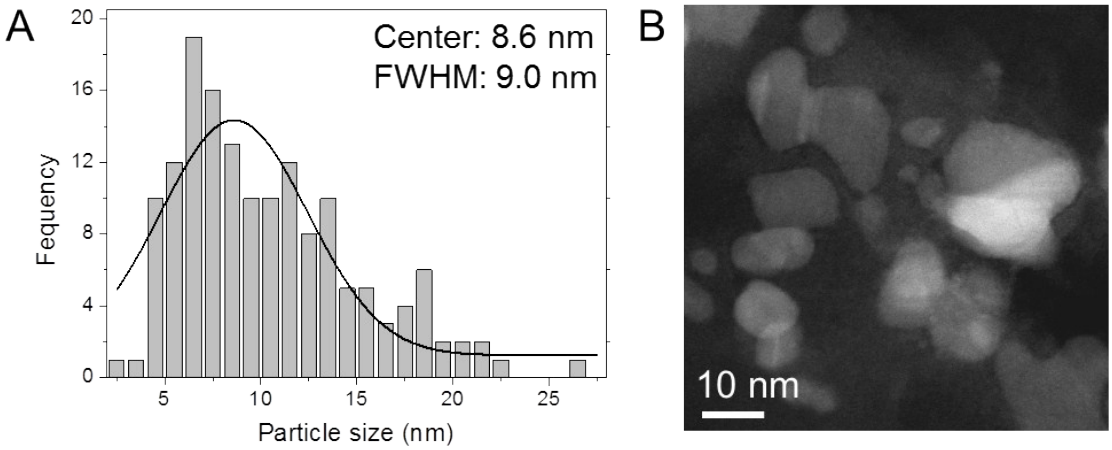

Figure S2: Particle size distribution from STEM image analysis and fitted with a Gaussian distribution function (A). The center of the distribution is 8.6 nm and the FWHM is 9.0 nm. An exemplary C_s-corrected STEM image of Ni@NiO nanoparticles, which was used for size distribution analysis (B).

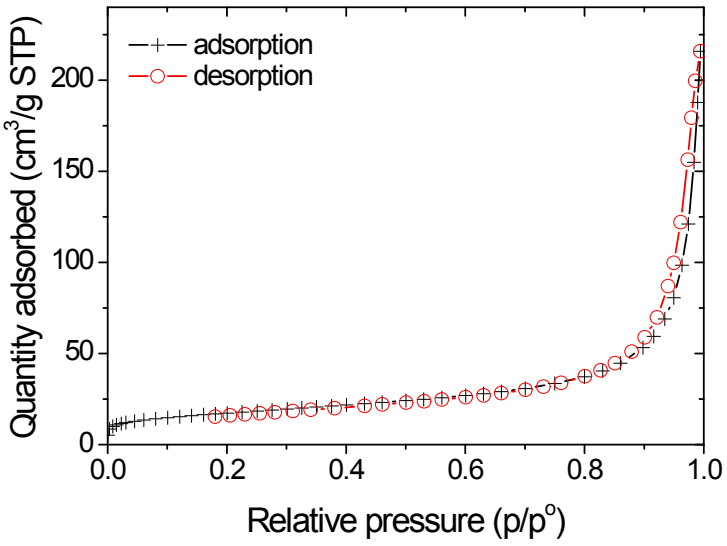

Figure S3 N_2 adsorption isotherm of C-Ni

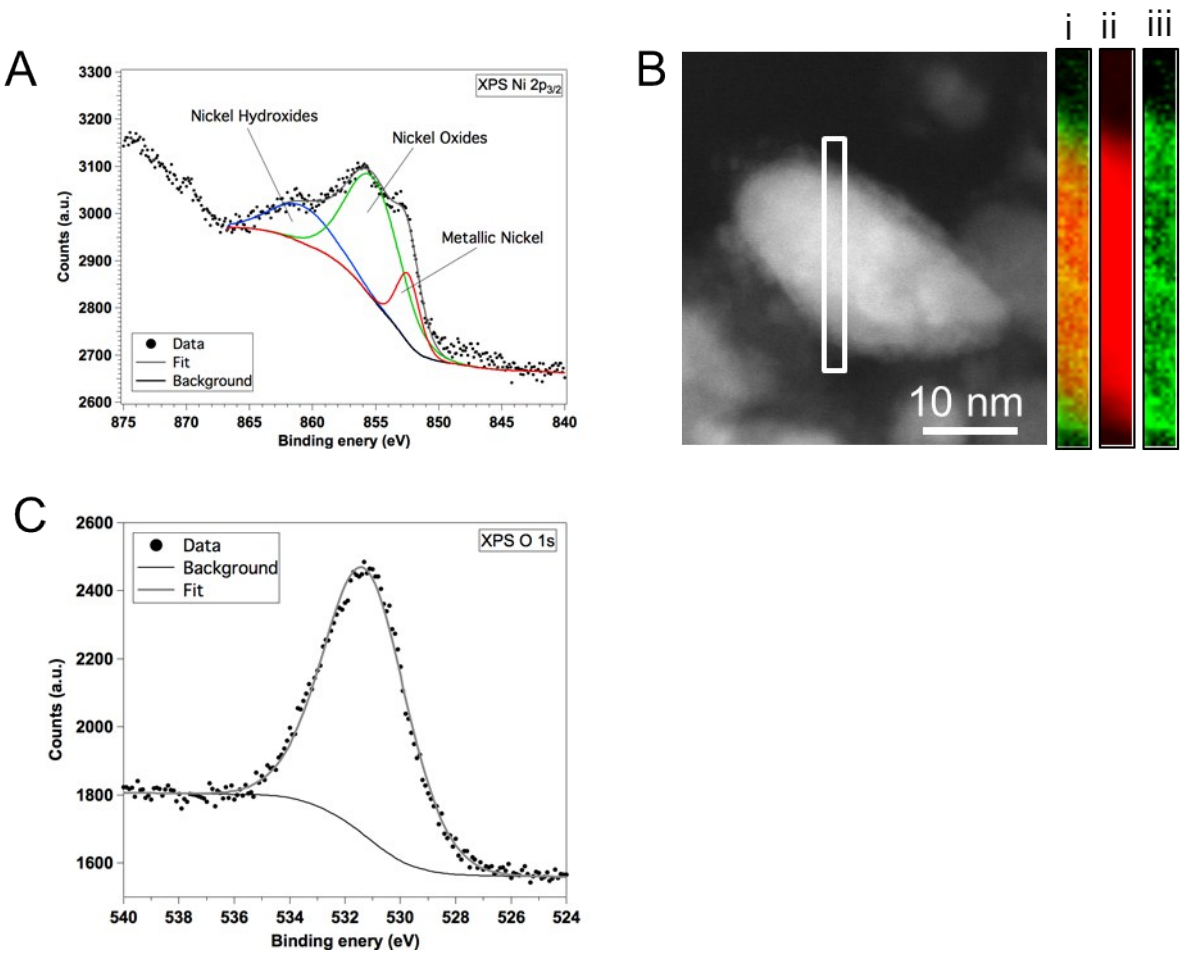

Figure S4. Ni 2p core level XPS spectrum of C-Ni shows three contributions at 852.4 eV, 855.1 eV and 860.8 eV binding energy, which can be attributed to metallic Ni, NiO, and NiOH, respectively [1] (A). C_s-corrected STEM micrograph and the corresponding EEL spectrum images (i,ii,iii) across a Ni@NiO nanoparticle (B). Color code: red refers to Ni-$L_{3,2}$ and green to O-K edges. EEL spectrum image i is an overlay of ii and iii. O 1s core level XPS spectrum of C-Ni showing a component located at 531.2 eV that has been attributed to crystal defects within the oxide [2] (C).

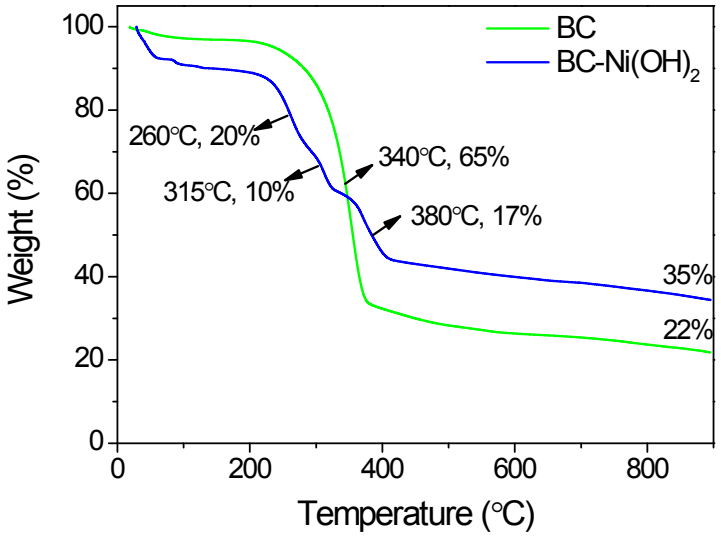

Figure S5. Thermogravimetric curves of BC and BC-Ni$(OH)_2$ in nitrogen.

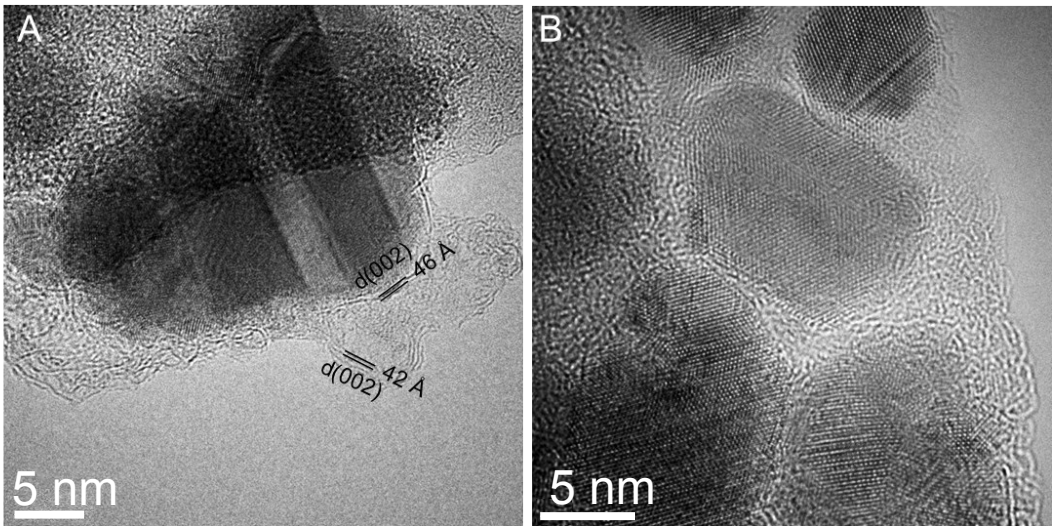

Figure S6. Cs-corrected TEM-BF micrographs of C-Ni showing Ni@NiO NPs covered by disordered graphite layers as suggested by the increased d(001) spacing of 42-46 Å (A). The NPs are embedded in a matrix of amorphous carbon (B).

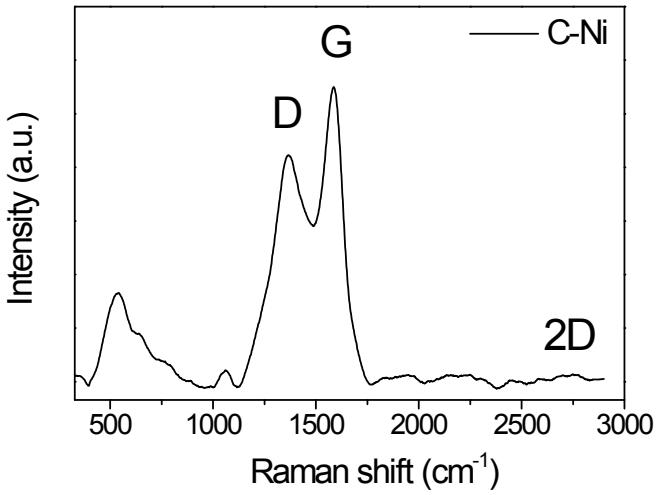

Figure S7. Raman spectrum of C-Ni showing the absence of the graphene 2D band at ~2700 cm^{-1}. The Raman spectrum was smoothed applying the Savitzky-Golay method with a 2nd polynomial order and 67 points of window.

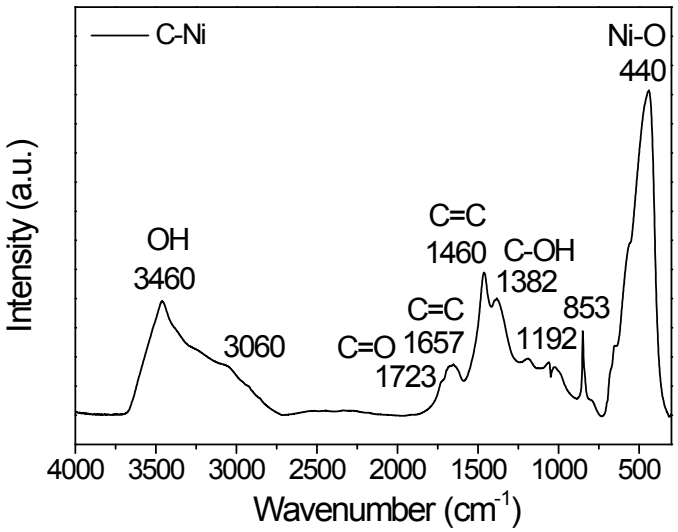

Figure S8. FTIR spectrum of C-Ni. The presence of functional carbon oxygen groups, i.e. C-O (1382 cm^{-1}) and C=O (1723 cm^{-1}), is observed together with indications of aromatic C=C groups (1460 cm^{-1}).

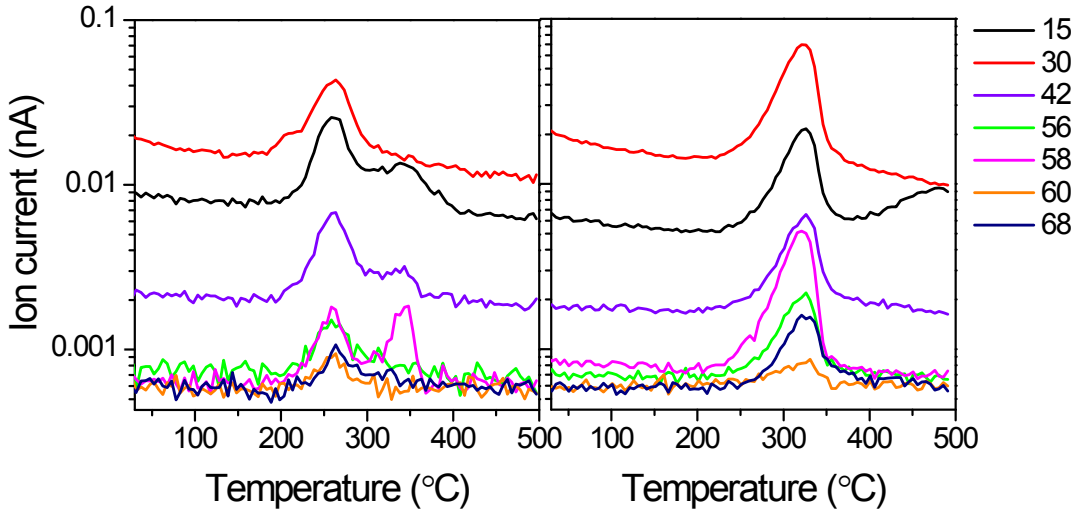

Figure S9. TG-MS curves of BC-$Ni(OH)_2$ (A) and BC (B) recorded in N_2 atmosphere. The curves correspond to ionized species with mass-to-charge ratios m/z of 15 (methyl); 30 (ethane); 42 (propene/ketene); 56 (2-propenal); 58 (ethanedione/propanone); 60 (acetic acid); 68 (furan). Species of m/z>68 did not evolve in significant quantity and remained below the quantity of furan.

In bacterial cellulose alone the decomposition products are generated in one temperature region around 325 °C, while in BC-$Ni(OH)_2$ at 260 °C and 340 °C. Interestingly, in the presence of $Ni(OH)_2$ the cellulose decomposition occurs about 70 °C below the decomposition temperature of pure bacterial cellulose. It is well-known that nickel compounds can catalyze the thermal decomposition of cellulose and other biomass and reduce the decomposition temperature [3,4].

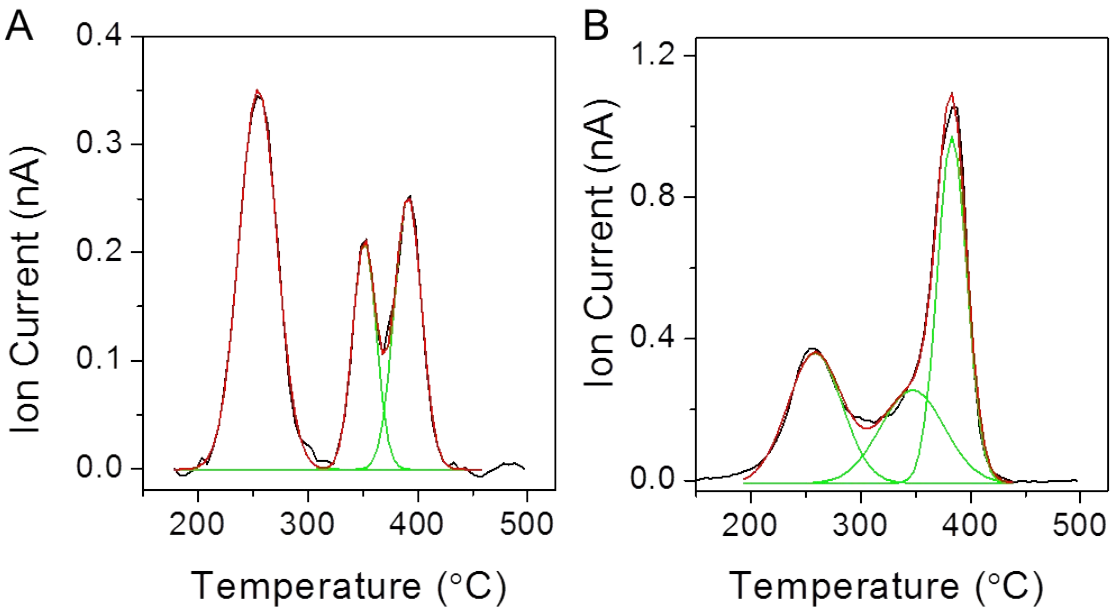

Figure S10: TG-MS curves of CO (A) and CO_2 (B) evolved from BC-$Ni(OH)_2$ under nitrogen. The green curves are Gaussian fits and the red curves are the envelope.

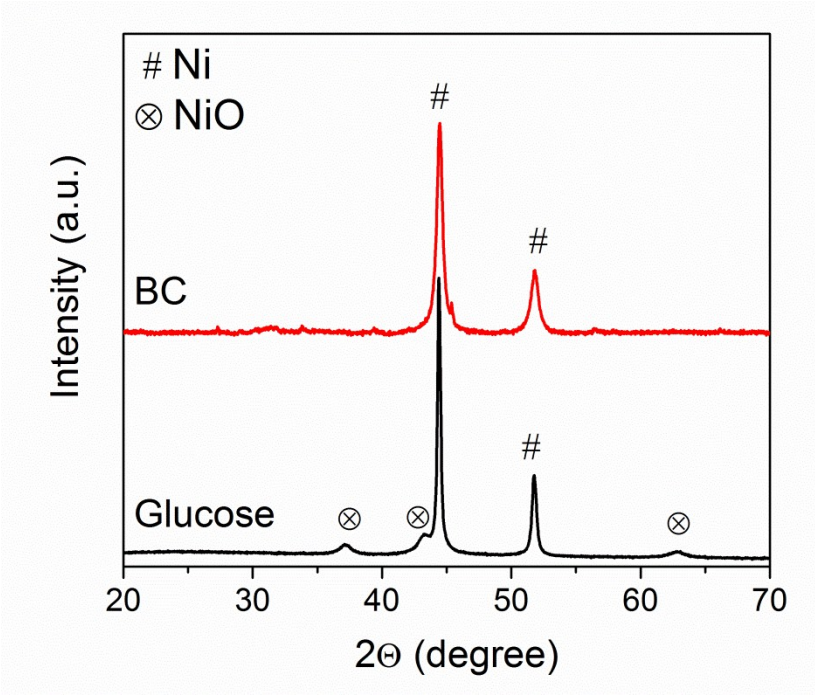

Figure S11: XRD pattern of Ni and a Ni/NiO mixture as obtained by carbothermal reduction of BC-$Ni(OH)_2$ and glucose-$Ni(OH)_2$, respectively.

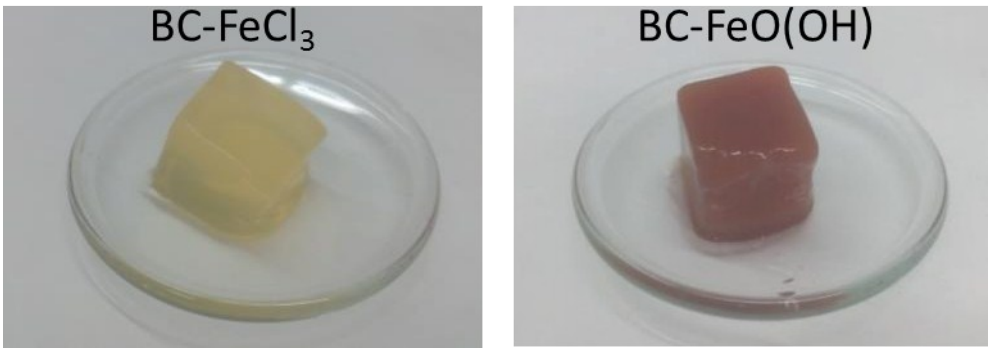

Figure S12: Photographs of a BC cube with infiltrated $FeCl_3$ (left) and the same cube after immersion in 1M NaOH for one hour (right), which provoked the precipitation of FeO(OH) within the BC cube.

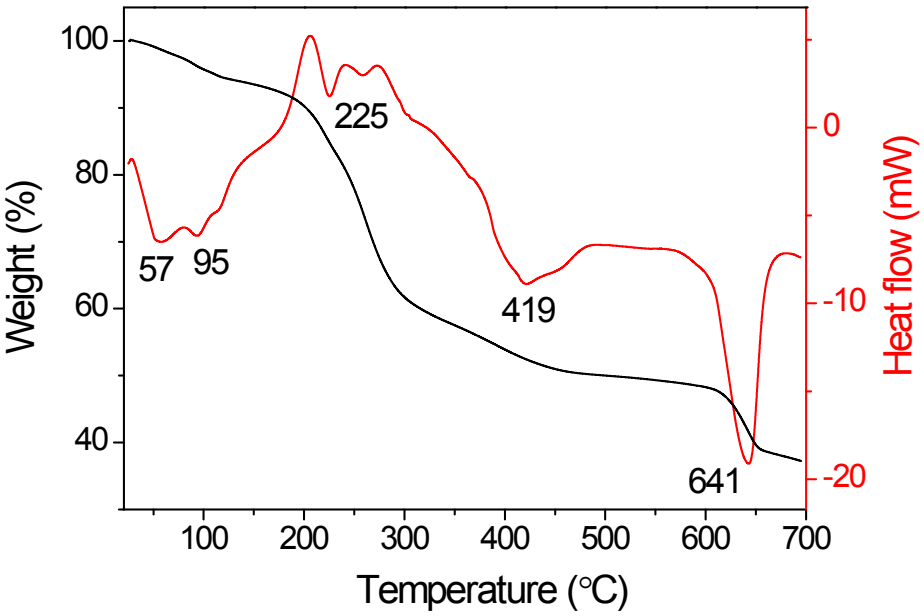

Figure S13: TG and DSC curves of BC-Fe(OH)$_3$ obtained under nitrogen atmosphere. The DSC peak at 641 °C can be attributed to the reduction of iron oxide to metallic Fe.

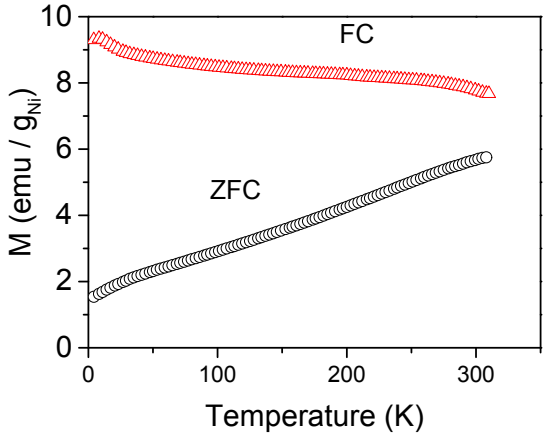

Figure S14: Plots of Zero Field Cooling (ZFC) – Field Cooling (FC) runs of the magnetization *versus* temperature, *M(T)*, as measured under 50k Oe cooling field and 50 Oe measuring field.

The ZFC and FC curves are widely separated from each other, which is a strong indication for magnetic anisotropy of the ferromagnetic phase. Furthermore, the blocking temperature, T_B, that is the transition from a magnetically blocked state to a superparamagnetic state, appears to be above 300 K as the ZFC curve does not show any peak in the measured temperature range. This behavior can be related to the

broad particles size distribution as observed in the TEM investigations and therefore, the superparamagnetic effect typically observed for Ni nanoparticles, is absent in C-Ni.

References

[1] A. P. Grosvenor, M. C. Biesinger, R. S. C. Smart, N. S. McIntyre, *Surf. Sci.* **2006**, *600*, 1771–1779.

[2] B. P. Payne, M. C. Biesinger, N. S. McIntyre, *J. Electron Spectros. Relat. Phenomena* **2009**, *175*, 55–65.

[3] J. Grams, N. Potrzebowska, J. Goscianska, B. Michalkiewicz, A. M. Ruppert, *Int. J. Hydrogen Energy* **2016**, *41*, 8656–8667.

[4] C. Wu, Z. Wang, J. Huang, P. T. Williams, *Fuel* **2013**, *106*, 697–706.